

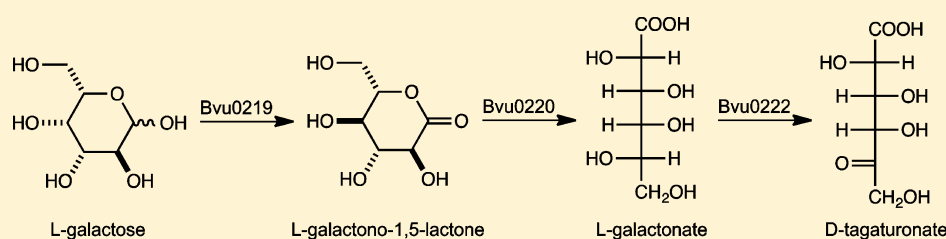
L-Galactose Metabolism in *Bacteroides vulgatus* from the Human Gut Microbiota

Merlin Eric Hobbs,[‡] Howard J. Williams,[§] Brandon Hillerich,[#] Steven C. Almo,[#] and Frank M. Raushel^{*,§,‡}

[‡]Department of Biochemistry and Biophysics, [§]Department of Chemistry, Texas A&M University, College Station, Texas 77843, United States

[#]Albert Einstein College of Medicine, 1300 Morris Park Avenue, Bronx, New York 10461, United States

S Supporting Information



ABSTRACT: A previously unknown metabolic pathway for the utilization of L-galactose was discovered in a prevalent gut bacterium, *Bacteroides vulgatus*. The new pathway consists of three previously uncharacterized enzymes that were found to be responsible for the conversion of L-galactose to D-tagaturonate. Bvu0219 (L-galactose dehydrogenase) was determined to oxidize L-galactose to L-galactono-1,5-lactone with k_{cat} and k_{cat}/K_m values of 21 s^{-1} and $2.0 \times 10^5 \text{ M}^{-1} \text{ s}^{-1}$, respectively. The kinetic product of Bvu0219 is rapidly converted nonenzymatically to the thermodynamically more stable L-galactono-1,4-lactone. Bvu0220 (L-galactono-1,5-lactonase) hydrolyzes both the kinetic and thermodynamic products of Bvu0219 to L-galactonate. However, L-galactono-1,5-lactone is estimated to be hydrolyzed 300-fold faster than its thermodynamically more stable counterpart, L-galactono-1,4-lactone. In the final step of this pathway, Bvu0222 (L-galactonate dehydrogenase) oxidizes L-galactonate to D-tagaturonate with k_{cat} and k_{cat}/K_m values of 0.6 s^{-1} and $1.7 \times 10^4 \text{ M}^{-1} \text{ s}^{-1}$, respectively. In the reverse direction, D-tagaturonate is reduced to L-galactonate with values of k_{cat} and k_{cat}/K_m of 90 s^{-1} and $1.6 \times 10^5 \text{ M}^{-1} \text{ s}^{-1}$, respectively. D-Tagaturonate is subsequently converted to D-glyceraldehyde and pyruvate through enzymes encoded within the degradation pathway for D-glucuronate and D-galacturonate.

Most of the microorganisms that colonize the human body reside within the gastrointestinal tract and are collectively known as gut microbiota. These microorganisms are of particular interest for the role they play in metabolism and human health.¹ While the human–microbiota relationship is predominantly commensal, there are reports implicating these microbes in a wide range of pathologies, including inflammatory bowel disease and colitis.² One important role for these organisms is the degradation of poorly digestible plant polysaccharides such as pectin, xylan, and cellulose.³ *Bacteroides* species are prevalent in the microbiota, and these organisms have been implicated as being partly responsible for the degradation of these polysaccharides. The various species of *Bacteroides* encode an unusually high number of glycoside hydrolases and polysaccharide lyases. *Bacteroides vulgatus* is thought to encode the largest number of enzymes targeting the degradation of pectin.^{3–5}

A cluster of genes that is likely responsible for an unknown metabolic pathway for the catabolism of carbohydrates in *B. vulgatus* is presented in Figure 1. Of the six genes identified in this cluster, four of them likely function to code for enzymes that utilize carbohydrate-based substrates. On the basis of

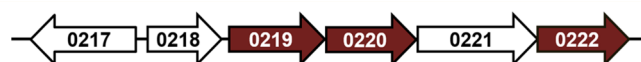


Figure 1. Genomic neighborhood of Bvu0220. Genes colored in maroon have been functionally characterized by this investigation and are as follows: Bvu0219 is L-galactose dehydrogenase, Bvu0220 is L-galactono-1,5-lactonase, and Bvu0222 is L-galactonate dehydrogenase. The genes in white are of unknown function. Bvu0217 is a putative glycoside hydrolase, Bvu0218 is a putative transcription regulator, and Bvu0221 is a putative sugar permease.

amino acid sequence identity to proteins of known function, Bvu0217 is a putative glycoside hydrolase from cog3669, Bvu0219 is a $\text{NAD}^+/\text{NADP}^+$ -dependent oxidoreductase from cog0667, Bvu0220 is a lactonase associated with cog3618, and Bvu0222 is a Zn^{2+} -dependent dehydrogenase from cog1063. The two remaining proteins, Bvu0218 and Bvu0221, appear to be a transcriptional regulator and a sugar permease from

Received: May 28, 2014

Revised: June 24, 2014

Published: June 25, 2014

cog0738, respectively. A potential metabolic pathway for these enzymes involves the initial hydrolysis of a more complex carbohydrate substrate (glycohydrolase), oxidation of the aldose product to a lactone (dehydrogenase), hydrolysis of the lactone to an acid sugar (lactonase), and the subsequent oxidation of the acid sugar (dehydrogenase).

Of the enzymes contained within this putative pathway for the catabolism of an unknown carbohydrate, we were particularly interested in the function of Bvu0220, a member of the amidohydrolase superfamily (AHS). The AHS is a diverse superfamily of enzymes that catalyzes a wide variety of reactions including the hydrolysis of amide or ester bonds, hydration, decarboxylation, and isomerization reactions.^{6–10} Most of the proteins in the AHS exhibit a distorted (β/α)₈-barrel topology, with the active site located at the C-terminal end of the β -barrel. Nearly all of the structurally characterized enzymes contained within the AHS bind one to three divalent cations, which are ligated to the protein via complexation with a common set of conserved amino acid residues. However, the structurally characterized lactonases from the AHS that are contained within cog3618 do not function with a divalent cation bound in the active site. The known lactonases from cog3618 include 2-pyrone-4,6-dicarboxylate lactonase (LigI), 4-sulfomuconolactonase (4-SML), L-rhamnonate-1,4-lactonase, and L-fucono-1,5-lactonase (FuL).^{11–13}

A sequence similarity network (SSN) for cog3618 calculated at a BLAST E-value of 10^{-30} is provided in Figure 2. Each node

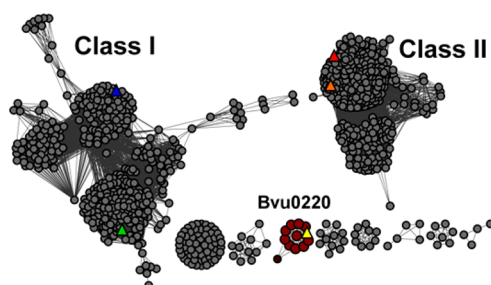


Figure 2. Sequence similarity network for cog3618 at an E-value of 10^{-30} where each node represents a protein and an edge represents an E-value between two proteins of 10^{-30} or smaller. The triangular nodes represent an enzyme with experimentally verified function. Nodes are color-coded as follows: LigI (red), 4-SML (orange), L-rhamnonate-1,4-lactonase (blue), FuL (green), and Bvu0220 (yellow).

within the sequence similarity network represents a unique protein contained within cog3618, which are connected to each other if they are related by an E-value of 10^{-30} or less. At this stringency level, cog3618 is subdivided into two primary groups, arbitrarily designated as Class I and Class II. Most of the enzymes within Class I are encoded adjacent to genes with an apparent relationship to carbohydrate metabolism.¹³ At this level of stringency, Bvu0220 is not associated with either Class I or Class II enzymes. Here we identify a novel metabolic pathway for the metabolism of L-galactose to D-tagaturonate. L-Galactose is first oxidized to L-galactono-1,5-lactone and then hydrolyzed to L-galactonate. This product is subsequently oxidized to D-tagaturonate, which is further metabolized to pyruvate and D-glyceraldehyde-3-phosphate.

MATERIALS AND METHODS

Materials. All chemicals and buffers were purchased from Sigma-Aldrich, unless otherwise specified. Sugar lactones that

were not commercially available were synthesized according to standard published procedures with the exception of 4-deoxy-L-fucono-1,5-lactone, which was enzymatically synthesized.^{13,14}

The noncommercial lactones included the following: L-fucono-1,4-lactone, D-arabinono-1,4-lactone, L-xylono-1,4-lactone, L-mannono-1,4-lactone, D-talono-1,4-lactone, D-allono-1,4-lactone, L-rhamnono-1,4-lactone, D-lyxono-1,4-lactone, L-lyxono-1,4-lactone, L-arabinono-1,4-lactone, D-xylono-1,4-lactone, L-mannono-1,5-lactone, L-rhamnono-1,5-lactone, and 4-deoxy-L-fucono-1,5-lactone. The sugar lactones that were obtained from either CarboSynth or ChromaDex included the following compounds: L-galactono-1,4-lactone, D-mannono-1,4-lactone, D-galactono-1,4-lactone, D-ribono-1,4-lactone, D-glucuro-6,3-lactone, D-erythronolactone, and L-glucono-1,5-lactone. Aldose sugars were obtained from either Sigma-Aldrich or CarboSynth and included L-fucose, L-galactose, L-glucose, D-altriose, D-arabinose, L-xylose, L-rhamnose, D-mannose, L-allose, D-talose, L-talose, D-allose, D-galactose, L-mannose, D-gulose, D-glucose, L-arabinose, L-ribose, D-lyxose, L-lyxose, D-xylose, D-ribose, and 4-deoxy-L-fucose.

Cloning, Expression and Purification of Bvu0220 from *B. vulgatus*. The gene for Bvu0220 (gil150002825; UniProt: A6KWY3) was amplified from *B. vulgatus* ATCC 8482 genomic DNA using 5'-TACTTCCAATCCATGATGGATTTTACATAATAGATGCACACTCC-3' as the forward primer and 5'-TATCCACCTTTACTGTTATTCTGACATGTTT-TTATGTAAGGAAGAGATATG-3' as the reverse primer. PCR was performed using KOD Extreme DNA Polymerase (Novagen). The conditions were 2 min at 95 °C, followed by 40 cycles of 20 s at 95 °C, 20 s at 66 °C, and 20 s at 72 °C. The amplified fragment was cloned into the N-terminal TEV cleavable 6x-His-tag containing vector, pNIC28-BSA, by ligation-independent cloning.¹⁵

The recombinant plasmid containing Bvu0220 was transformed into BL21 (DE3) cells (Novagen), via electroporation. Five milliliter cultures of LB medium supplemented with 50 $\mu\text{g}/\text{mL}$ kanamycin were inoculated with a single colony and grown overnight at 37 °C. Overnight cultures were used to inoculate 1 L of LB medium (50 $\mu\text{g}/\text{mL}$ kanamycin) and incubated at 37 °C until an OD₆₀₀ of 0.4–0.6 was achieved. Gene expression was induced by the addition of 0.1 mM isopropyl β -thiogalactoside (IPTG) at ambient temperature for 18 h. Cells were harvested via centrifugation at 8000 rpm at 4 °C. Cell pellets were resuspended in purification buffer (50 mM HEPES, 500 mM NaCl, 40 mM imidazole, 0.1 mg/mL phenylmethanesulfonyl fluoride, pH 7.5) and lysed via multiple rounds of sonication. Nucleic acids were removed from the cell lysate with the addition of 2% (w/v) protamine sulfate over 30 min at 4 °C, followed by centrifugation (8000 rpm). The resulting supernatant was applied to a 5 mL HisTrap HP (GE Healthcare) nickel affinity column. Protein was eluted from the nickel affinity column with 50 mM HEPES (pH 7.5), 0.5 M NaCl, and 500 mM imidazole over a gradient of 23 column volumes.

Cloning, Expression, and Purification of Bvu0219 and Bvu0222 from *B. vulgatus*. The gene for Bvu0219 (gil150002825; UniProt: A6KWY2) was cloned from *B. vulgatus* ATCC 8482 with the primer pair 5'-ATGAATTACAATGAAATGGGAAAACCGGTATGCGGGTT-3' and 5'-TGAA-TTAGCCCAACTGATACGCATTTGTTTCCGATAA-3'. Restriction sites for NheI and XhoI were inserted into the forward and reverse primers. The PCR product was purified with a Promega PCR cleanup system and subsequently digested

with NheI and HindIII. The resulting DNA product was ligated into a pET-24a(+) vector (Novagen). The ligation reaction mixture was transformed into BL21(DE3) cells via electroporation. A single colony containing the plasmid of interest was used to inoculate 5 mL overnight cultures of LB (50 $\mu\text{g}/\text{mL}$ kanamycin) and incubated at 37 °C. One liter cultures of LB containing 50 $\mu\text{g}/\text{mL}$ kanamycin were inoculated with a 5 mL overnight culture and then grown at 37 °C until an OD_{600} of 0.4–0.6 was obtained. The cultures were transferred to ambient temperature, and gene expression was initiated with the addition of 1.0 mM isopropyl IPTG. Cells were harvested after 18 h via centrifugation at 4 °C and suspended in 50 mM HEPES (pH 7.5), 0.25 mM NaCl, and 0.1 mg/mL of PMSF. Resuspended cells were lysed via multiple rounds of sonication, and cell debris was removed via centrifugation at 4 °C. Nucleic acids were removed from the supernatant solution with the dropwise addition of 2% (w/v) protamine sulfate at 4 °C. Protamine sulfate-bound DNA was removed by centrifugation. Ammonium sulfate was added between 30 and 50% saturation, and the precipitated protein was isolated by centrifugation. The protein was resuspended in 20 mM HEPES (pH 7.5) and then applied to a High Load 26/60 Superdex 200 gel filtration column (GE Healthcare). Fractions containing the protein of expected size were pooled and purified further by ion exchange chromatography with a ResourceQ column (6 mL) at pH 7.5.

The gene coding for Bvu0222 (gil149931251; UniProt: A6KWY5) was determined to contain 19 rare codons using the Rare Codon Calculator (RaCC) (nihserver.mbi.ucla.edu/RACC/).¹⁶ A codon-optimized gene was purchased from GenScript, which was ligated into a pUC57 cloning vector containing NdeI and HindIII restriction sites. The plasmid harboring the gene of interest was digested with NdeI and HindIII at 37 °C for 3 h. The resulting gene was ligated into pET-32a (+) (Novagen) and transformed into BL21(DE3) cells via electroporation. The purification of Bvu0222 was conducted in manner similar to that described for Bvu0219. The isolation of uronate isomerase (URI) from *Escherichia coli* and L-fucose dehydrogenase (FucD) from *Burkholderia multivorans* (BmulJ_04919) was conducted as previously described.^{13,17}

Measurement of Enzyme Activity. The enzymatic hydrolysis of lactones by Bvu0220 was monitored with a SpectraMax340 UV–visible using a colorimetric pH indicator assay at 30 °C, as previously described.¹³ Protons released during the hydrolysis of lactones were measured using the pH indicator bromothymol blue. Reaction mixtures contained 2.5 mM MOPS (pH 7.1), 0.2 M NaCl, 0–0.5 mM lactone, and 0.1 mM bromothymol blue in a final volume of 250 μL . The final concentration of DMSO was 1%. Changes in absorbance at 616 nm ($\epsilon = 1135 \text{ M}^{-1} \text{ cm}^{-1}$) were monitored in 96-well plates. The background rate arising from acidification of the reaction mixture by atmospheric CO_2 was subtracted from the initial rates.

The dehydrogenase activities of Bvu0222 and Bvu0219 were monitored by following the reduction of NAD^+ or NADP^+ at 340 nm ($\epsilon = 6220 \text{ M}^{-1} \text{ cm}^{-1}$) at 30 °C with a SpectraMax340 UV–visible spectrophotometer. Reaction assays for Bvu0219 were performed in 50 mM BICINE buffer (pH 8.0), varying concentrations of substrate, and 0.5 mM NADP^+ . Reaction assays for Bvu0222 were conducted in 50 mM phosphate buffer at pH 7.5. Kinetic constants for NADP^+ were determined with 200 μM substrate and variable concentrations of NADP^+ (0–1.5 mM).

The reductase activity of Bvu0222 was monitored using a coupled assay system. The coupling system consisted of 8.0 μM URI, D-galacturonate (0–4 mM), 50 mM phosphate buffer (pH 7.0), NADH (1.0 mM), and Bvu0222. The reactions were allowed to incubate for 15 min in the absence of Bvu0222 at 30 °C to allow for the URI catalyzed isomerization of D-galacturonate to D-tagaturonate. Reactions were initiated by the introduction of Bvu0222 and monitored through the oxidation of NADH at 340 nm at 30 °C, with a SpectraMax340 UV–visible spectrophotometer.

Data Analysis. The kinetic constants were determined from a fit of the initial velocity data to eq 1 using SigmaPlot 9, where v is the initial velocity, E_t is the total enzyme concentration, k_{cat} is the turnover number, $[A]$ is the substrate concentration, and K_m is the Michaelis constant.

$$v/E_t = k_{\text{cat}}[A]/(K_m + [A]) \quad (1)$$

Metal Analysis. The metal content of Bvu0220 and Bvu0222 was determined using an Elan DRC II ICP-MS instrument as previously described.¹⁸ Protein samples for ICP-MS analysis were digested with HNO_3 and then refluxed for 30 min.¹⁹ All buffers were passed through a column of Chelex 100 (Bio-Rad) to remove trace metal contamination. EDTA and 1,10-phenanthroline (1.0 mM) were incubated with 1.0 μM Bvu0220 in 50 mM buffer at various pH values ranging from 6 to 10 to remove divalent metal ions, as previously described.¹³ The following buffers were used: CHES (pH 6.0), HEPES (pH 7.0), BICINE (pH 8.0), and CHES (pH 9.0 and 10.0). The effect of added divalent cations on the catalytic activity of Bvu0220 was determined by supplementing Mn^{2+} , Zn^{2+} , Co^{2+} , Cu^{2+} , or Ni^{2+} (0–500 μM) directly to the assay mixtures. The purified enzyme was also incubated with 50–500 mol equiv of these divalent cations for 24 h at 4 °C in 50 mM HEPES (pH 7.5) and subsequently assayed for catalytic activity.

Identification of Reaction Product of L-Galactose Oxidation Catalyzed by Bvu0219. The product of the reaction catalyzed by Bvu0219 was determined by ^{13}C NMR spectroscopy using a Bruker Avance III 500 MHz spectrometer equipped with a 5 mm HCN cryoprobe. The reaction sample contained 250 mM phosphate (pH 5.8), 10% D_2O , 10 mM NAD^+ , 10 mM [^{13}C -1]-L-galactose (Omicron Biochemicals) and 10–50 μM Bvu0219 in a volume of 250 μL . The reaction was initiated by the addition of Bvu0219 and terminated at 10 min by removal of the enzyme by passage through a 3 kDa cutoff VWR centrifugal filter. The pH of the sample was adjusted to 7.0 to facilitate the nonenzymatic transformation of L-galactono-1,5-lactone to the thermodynamically more stable L-galactono-1,4-lactone.

Hydrolysis of L-Galactono-1,5-Lactone by Bvu0220. L-Galactono-1,5-lactone was identified as the preferred substrate for Bvu0220 via ^{13}C NMR spectroscopy. The reaction was initiated by the addition of 50 μM Bvu0219 to a solution containing 250 mM phosphate (pH 5.8), 10% D_2O , 10 mM NAD^+ , and 10 mM [^{13}C -1]-L-galactose. The reaction was monitored by ^{13}C NMR spectroscopy until the resonances for the 1,4- and 1,5-lactones of L-galactose were approximately equal. At this point, 1.0 μM Bvu0220 was added, and the ^{13}C NMR spectra were collected as a function of time.

Enzymatic Synthesis of Acid Sugars and Lactones. The acid sugars of L-galactose and L-glucose were synthesized enzymatically from L-galactono-1,4-lactone and L-glucono-1,5-lactone using Bvu0220 as the catalyst. Reaction conditions were as follows: 50 mM lactone, 50 mM carbonate buffer (pH 9.5),

Scheme 1

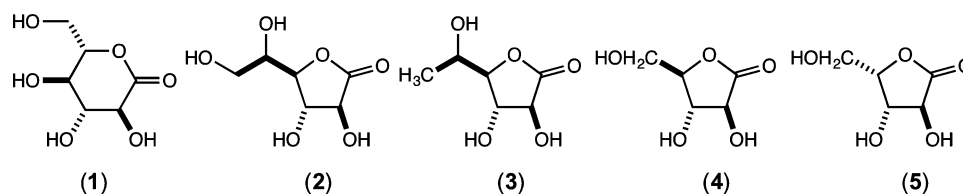


Table 1. Catalytic Constants for Bvu0220, Bvu0219, and Bvu0222

enzyme	substrate	k_{cat} (s^{-1})	K_m (μM)	k_{cat}/K_m ($\text{M}^{-1} \text{s}^{-1}$)
Bvu0220 ^a	L-glucono-1,5-lactone (1)	38 ± 1	500 ± 40	(8.0 ± 0.5) × 10 ⁴
	L-galactono-1,4-lactone (2)	34 ± 3	1950 ± 310	(1.8 ± 0.2) × 10 ⁴
	L-fucono-1,4-lactone (3)	23 ± 2	1320 ± 210	(1.8 ± 0.2) × 10 ⁴
	4-deoxy-L-fucono-1,5-lactone (12)	23 ± 1	32 ± 4	(7.2 ± 0.8) × 10 ⁵
	L-xylo-1,4-lactone (5)	5.3 ± 0.4	5500 ± 550	(9.3 ± 0.4) × 10 ²
Bvu0219 ^b	D-arabino-1,4-lactone (4)	1.0 ± 0.1	1700 ± 140	(5.0 ± 0.3) × 10 ²
	L-galactose (6)	21 ± 1	109 ± 4	(2.0 ± 0.1) × 10 ⁵
	L-glucose (7)	ND ^e	ND	(2.0 ± 0.2) × 10 ²
	D-arabinose (8)	ND	ND	(7.1 ± 0.1) × 10 ¹
	L-fucose (9)	ND	ND	(3.4 ± 0.1) × 10 ¹
	D-altrose (10)	ND	ND	(1.3 ± 0.1) × 10 ¹
	NADP ⁺ (with L-galactose)	22 ± 1	3.0 ± 0.5	(8.0 ± 0.4) × 10 ⁶
	NAD ⁺ (with L-galactose)	25 ± 1	3000 ± 200	(9.0 ± 0.1) × 10 ³
Bvu0222 ^c	L-galactonate (13)	0.6 ± 0.1	36 ± 3	(1.7 ± 0.1) × 10 ⁻⁴
	L-gluconate (14)	0.2 ± 0.1	510 ± 70	(3.9 ± 0.6) × 10 ²
	L-fuconate	ND	ND	(2.0 ± 0.1) × 10 ²
	D-tagaturonate (15) ^d	90 ± 0.6	550 ± 50	(1.6 ± 0.2) × 10 ⁵

^aBromothymol blue pH indicator assay and MOPS (pH 7.1). ^b50 mM BICINE buffer (pH 8.0), varying concentrations of substrate and 0.5 mM NADP⁺. ^c50 mM phosphate buffer (pH 7.5) varying concentrations of substrate and 0.5 mM NAD⁺. ^d50 mM phosphate buffer (pH 7.0) varying concentrations and 1.0 mM NADH. ^eND, did not determine because the enzyme was not saturated at the highest substrate concentration employed.

and 20 μM Bvu0220 were incubated together overnight. 4-Deoxy-L-fucono-1,5-lactone was synthesized enzymatically from 4-deoxy-L-fucose using FucD as previously described.¹³ The reaction was conducted in 50 mM phosphate buffer (pH 7.0) containing 15 mM 4-deoxy-L-fucose, and 15 mM NAD⁺ in a final volume of 1.0 mL for 20 min.

Sequence Similarity Network for cog3618. Approximately 2000 proteins belonging to cog3618 were identified from the NCBI protein database using the query “cog3618”. The proteins within cog3618 were subjected to an all-by-all BLAST at a specified *E*-value (10⁻⁵⁰, 10⁻⁶⁰, etc.) using the NCBI standalone BLAST program. The BLAST files were opened and visualized in the similarity network program Cytoscape.^{20,21}

Multiple Sequence Alignment. FASTA sequence files were obtained from the NCBI Protein database for Bvu0220, LigI, and FucL. Multiple sequence alignments were prepared using JalView 2.8.0.²²

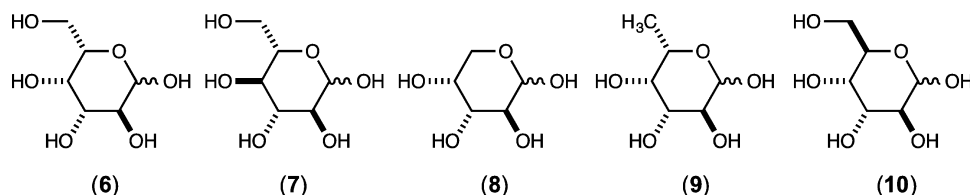
RESULTS

Functional Characterization of Bvu0220. The gene encoding Bvu0220 from *B. vulgatus* was cloned and expressed in *E. coli*, and the protein purified to homogeneity. The as-purified Bvu0220 contained ~0.3 mol equiv of Mn²⁺, 0.1 mol equiv of Fe²⁺, and 0.3 mol equiv of Ni²⁺. The metal ions were removed by incubation of the enzyme with EDTA and *o*-phenanthroline overnight. Since other enzymes from cog3618

have been shown previously to hydrolyze γ - and δ -lactones of acid sugars, Bvu0220 was incubated with a small library of 25 acid sugar lactones as a preliminary test of catalytic activity. Of the compounds tested, hydrolysis was detected only with L-glucono-1,5-lactone (1), L-galactono-1,4-lactone (2), L-fucono-1,4-lactone (3), D-arabino-1,4-lactone (4), and L-xylo-1,4-lactone (5). The structures of these compounds are illustrated in Scheme 1. The activity of Bvu0220 was not affected by the addition of chelating agents, or the addition of Mn²⁺, Zn²⁺, Co²⁺, Cu²⁺, or Ni²⁺ directly to the assay mixture. From these results, we concluded that Bvu0220 is not dependent on the binding of divalent cations for catalytic activity and that the function of this enzyme is to hydrolyze lactones of acid sugars. The kinetic constants for the hydrolysis of lactones 1 through 5 by Bvu0220 are presented in Table 1. L-Glucono-1,5-lactone was the best of these substrates with a value of k_{cat}/K_m of 8 × 10⁴ M⁻¹ s⁻¹.

Functional Characterization of Bvu0219. The gene for Bvu0219 is adjacent to the gene for Bvu0220. This protein is currently annotated as an “oxidoreductase” from cog0667, and the functionally characterized enzymes from cog0667 include dehydrogenases for the oxidation of L-fucose and D-arabinose. Bvu0219 also shares significant sequence identity (42–46%) to L-galactose dehydrogenase from two plants species, ornamental tobacco (*Nicotiana langsdorffii* × *Nicotiana sandera*) and *Arabidopsis thaliana*. It was therefore predicted that Bvu0219 would oxidize a monosaccharide to the corresponding lactone

Scheme 2



and that the product of the reaction catalyzed by Bvu0219 would be the physiological substrate for the lactonase activity of Bvu0220. Bvu0219 was screened against a substrate library of 23 commercially available pentose and hexose sugars by following the reduction of NADP^+ at 340 nm. Catalytic activity was observed for L-galactose (6), L-glucose (7), D-arabinose (8), L-fucose (9), and D-altrose (10) using NADP^+ as the oxidant. The structures of these compounds are presented in Scheme 2, and the kinetic constants are presented in Table 1. L-Galactose is the best substrate identified for Bvu0219 with a value of k_{cat}/K_m of $2 \times 10^5 \text{ M}^{-1} \text{ s}^{-1}$. The rate constants for the other substrates are reduced by more than 3 orders of magnitude.

Identification of the Initial Reaction Product of Bvu0219. Previous reports have suggested that the reaction product for the oxidation of L-galactose is L-galactono-1,4-lactone (2) rather than L-galactono-1,5-lactone (11).^{23–26} L-Galactose dehydrogenase activity has previously been reported in plant species, where this reaction is important for the biosynthesis of ascorbic acid.²⁷ It is likely that the initial product is actually L-galactono-1,5-lactone (11) since the pyranose form of L-galactose is the predominant configuration in solution.²⁸ However, L-galactono-1,5-lactone (11) has not been observed previously due to its chemical instability and nonenzymatic rearrangement to L-galactono-1,4-lactone (2). We therefore attempted to determine the structure of the initial oxidation product in the reaction catalyzed by Bvu0219 by NMR spectroscopy using [^{13}C -1]-L-galactose. The enzymatic reaction was conducted at pH 5.8 to help stabilize the initial oxidation product.¹³

The ^{13}C NMR spectrum for [^{13}C -1]-L-galactose is presented in Figure 3A. The four resonances correspond to C-1 for each of the four anomers of L-galactose. The chemical shifts of the α - and β -pyranose forms are observed at 96.5 and 92.3 ppm, respectively. The α - and β -furanose anomers are found at 95.0 and 101.0 ppm, respectively. The anomeric ratios are consistent with data reported by Angyal and Pickles: β -pyranose (64%), α -pyranose (29%), β -furanose (4%), and α -pyranose (3%).²⁸ After Bvu0219 is added to a mixture of NAD^+ and [^{13}C -1]-L-galactose at pH 5.8, a new resonance begins to appear at 174.1 ppm. Over a period of 15 min, the resonance at 174.1 ppm diminishes and a new resonance begins to appear at 175.9 ppm (Figure 3B). The resonance at 175.9 ppm is assigned to that of L-galactono-1,4-lactone (2) based on a direct comparison with the chemically synthesized material. The transient resonance that appears at 174.1 ppm is that of L-galactono-1,5-lactone (11). Therefore, the initial product of the reaction catalyzed by Bvu0220 is L-galactono-1,5-lactone (11). This unstable product is nonenzymatically converted to L-galactono-1,4-lactone (2) with an estimated rate constant of $\sim 0.2 \text{ min}^{-1}$ at pH 7.0.

Identification of the Physiological Substrate for Bvu0220. The best substrate for Bvu0219 is clearly L-galactose, but the best substrate for Bvu0220 is not the corresponding L-galactono-1,4-lactone (2). To determine if the best substrate for Bvu0220 is actually the chemically unstable L-galactono-1,5-

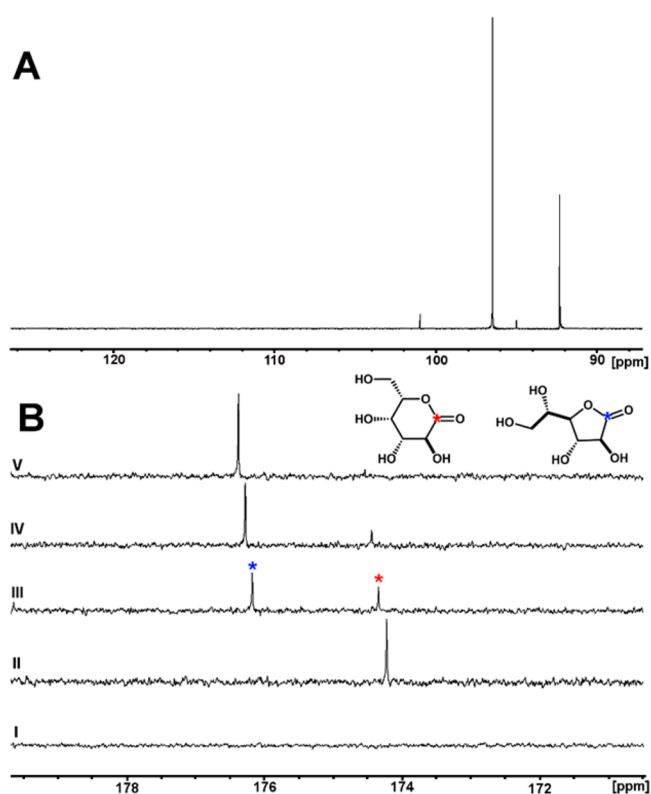


Figure 3. ^{13}C NMR spectra for [^{13}C -1]-L-galactose and the nonenzymatic transformation of L-galactono-1,5-lactone (11) to L-galactono-1,4-lactone (2). (A) The four ^{13}C -resonances correspond to the anomeric carbon for each of the four anomers of L-galactose (6). Chemical shifts are as follows: α -pyranose (92.3 ppm), β -pyranose (96.5 ppm), α -furanose (95.0 ppm), and β -furanose (101.0 ppm). (B) (I) The carbonyl region of L-galactose (6) is presented at time 0. (II) Bvu0219 added with L-galactono-1,5-lactone (11) as the predominate species (174.1 ppm). The enzyme was removed and the pH adjusted to 7. (III) The resonance signal for L-galactono-1,5-lactone decreases as the signal for L-galactono-1,4-lactone (175.9 ppm) increases in the absence of enzyme. (IV) After 10 min the predominant species is L-galactono-1,4-lactone (2). (V) After 15 min all of the L-galactono-1,5-lactone has been converted to L-galactono-1,4-lactone.

lactone (11), Bvu0219 was incubated with [^{13}C -1]-L-galactose and NAD^+ at pH 5.8, and the reaction was monitored via ^{13}C NMR spectroscopy (Figure 4). After 15 min the resonances for both lactones were approximately equal in intensity (Figure 4C). Bvu0220 was then added to the reaction mixture, and the ^{13}C NMR spectrum was monitored as a function of time (Figure 4D). The resonance at 174.1 ppm, corresponding to L-galactono-1,5-lactone (11), disappeared rapidly, and a new resonance appeared at 179.4 ppm, which corresponds to the hydrolysis product, L-galactonate (13). Similarly, when both enzymes (Bvu0219 and Bvu0220) were added to a mixture of NAD^+ and [^{13}C -1]-L-galactose at pH 5.8, the resonance for L-

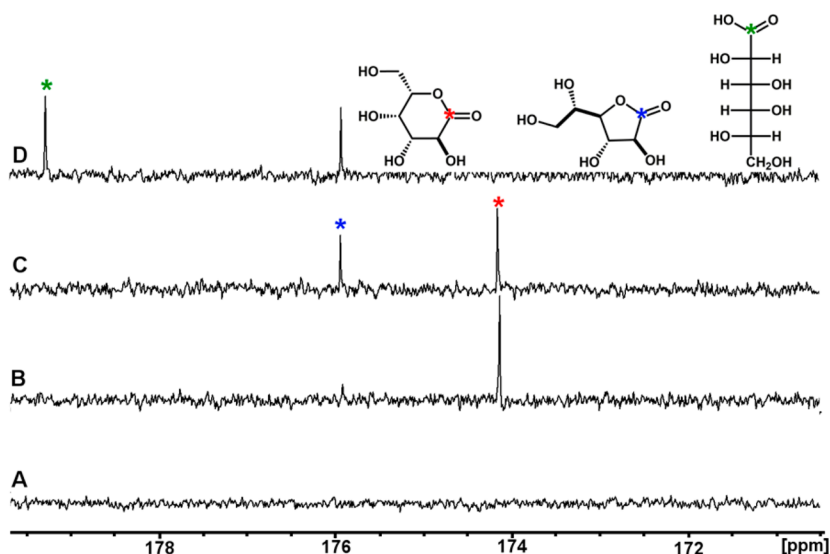
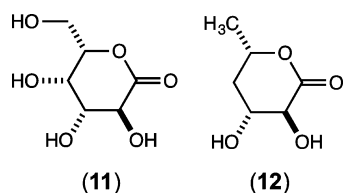


Figure 4. ^{13}C NMR analysis of the reactions catalyzed by Bvu0219 and Bvu0220 utilizing ^{13}C -1-L-galactose as substrate. (A) The carbonyl region of ^{13}C -1-L-galactose. (B) The predominate species after the addition of Bvu0219 is L-galactono-1,5-lactone (174.1 ppm, red asterisk). (C) 10 min after the addition of Bvu0219 the resonances corresponding to C-1 of L-galactono-1,5-lactone and L-galactono-1,4-lactone (175.9 ppm, blue asterisk) are approximately equal. At this point Bvu0220 was added to the reaction mixture. (D) 5 min after the addition of Bvu0220, L-galactono-1,5-lactone has disappeared. A new resonance with a chemical shift of 179.4 ppm appeared, which corresponds to L-galactonate (green asterisk).

galactono-1,4-lactone (2) was not observed. The only resonance that was observed was that for L-galactonate (13) at 179.4 ppm (data not shown). We estimate by NMR spectroscopy that Bvu0220 hydrolyzes L-galactono-1,5-lactone (11) 300 times faster than L-galactono-1,4-lactone (2). Therefore, the likely physiological substrate for Bvu0220 is L-galactono-1,5-lactone (11) that results from the oxidation of L-galactose (6) by Bvu0219 (Scheme 3).

Scheme 3

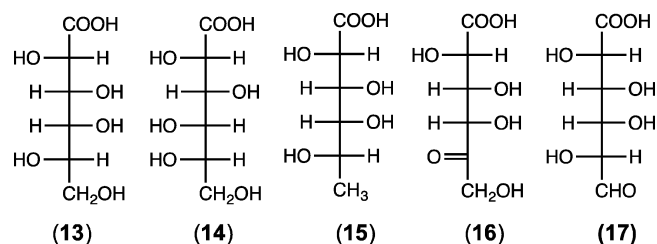


To further investigate the preferential hydrolysis of 1,5-lactones by Bvu0220, 4-deoxy-L-fucono-1,5-lactone (12) was synthesized enzymatically using L-fucose (9) and L-fucose dehydrogenase (FucD). This lactone is missing the hydroxyl group at C-4 and therefore cannot rearrange to a 1,4-lactone. The enzymatic product, 4-deoxy-L-fucono-1,5-lactone (12), was confirmed through ^1H NMR spectroscopy (data not shown). The 4-deoxy-L-fucono-1,5-lactone (12) was isolated, and the kinetic constants for the hydrolysis by Bvu0220 were determined at pH 7.1. The value of k_{cat}/K_m for the hydrolysis of 4-deoxy-L-fucono-1,5-lactone (12) is approximately an order of magnitude greater than that for L-glucono-1,5-lactone (1) and almost 2 orders of magnitude greater than for L-fucono-1,4-lactone (3).

Functional Characterization of Bvu0222. The gene for Bvu0222 is adjacent to Bvu0219 and Bvu0220, and this protein is currently annotated as a Zn^{2+} -dependent oxidoreductase from cog1063. Functionally characterized members of cog1063 include L-threonine dehydrogenase, L-idonate dehydrogenase, and sorbitol dehydrogenase. The closest homologue with an

experimentally determined catalytic function is LgnH (gil 425703034, UniProt K7ZKU8) from *Paracoccus* sp. 43P, with a sequence identity of 46%. The gene for LgnH is contained in an operon for the catabolism of the rare sugar L-glucose. LgnH has been reported to oxidize L-galactonate (13) and L-gluconate (14) at approximately the same rate.²⁹ Bvu0222 catalyzes the oxidation of L-galactonate (13), L-gluconate (14), and L-fuconate (15); however, the value of k_{cat}/K_m for the oxidation of L-galactonate (13) is 2 orders of magnitude greater than the oxidation of L-gluconate (14) (Table 1). D-Arabinonate and L-xylonate were also assayed for activity; however, no oxidation was detected. The oxidation product of L-galactonate (13) by Bvu0222 was confirmed to be D-tagaturonate (16). D-Tagaturonate (16) was prepared by the isomerization of D-galacturonate (17) by the enzyme uronate isomerase.¹⁷ The kinetic constants for the reduction of D-tagaturonate (16) are presented in Table 1, and the structures of compounds 13 through 17 are presented in Scheme 4.

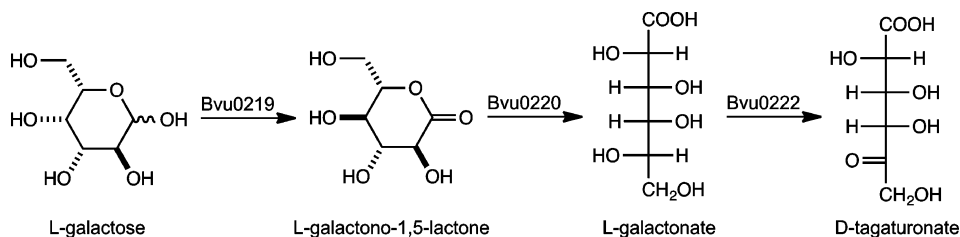
Scheme 4



DISCUSSION

Novel Metabolic Pathway for L-Galactose. The three enzymes from *B. vulgatus* examined in this study function to form a previously unknown pathway for the metabolism of L-galactose (6). The first enzyme in the pathway, Bvu0219, preferentially oxidizes L-galactose (6) to L-galactono-1,5-lactone (11) using NADP^+ as the oxidant with a k_{cat}/K_m of $>10^5 \text{ M}^{-1}$

Scheme 5



Scheme 6

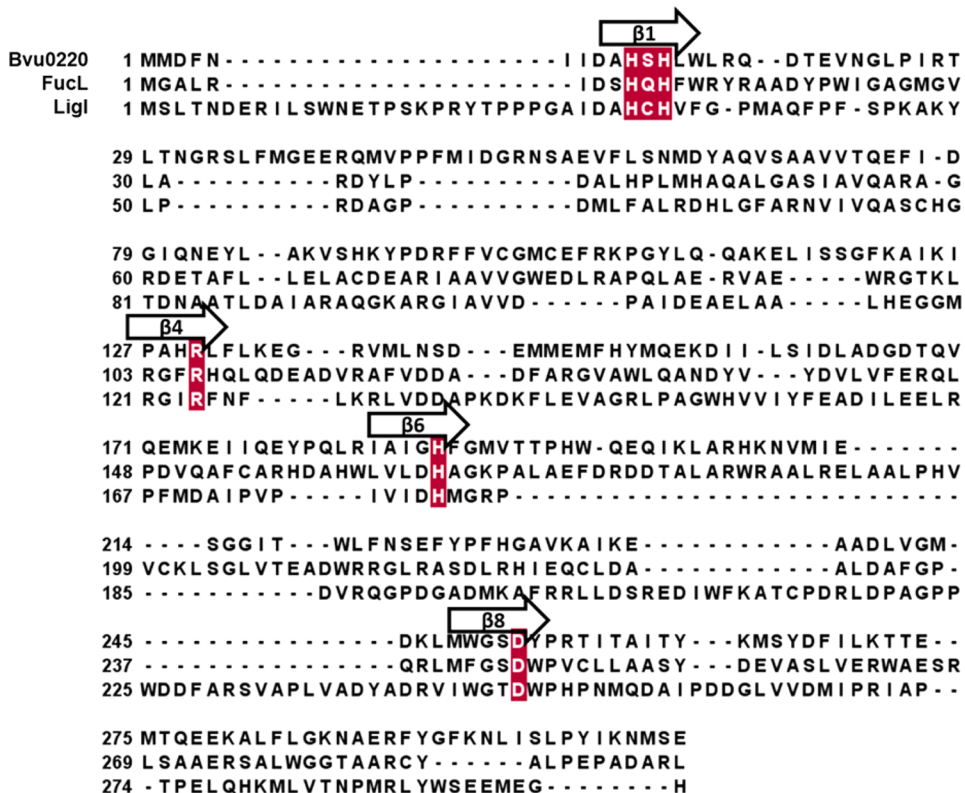
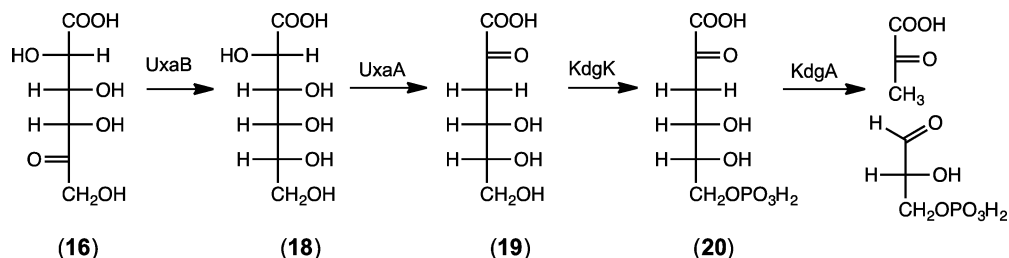


Figure 5. Sequence alignment of Bvu0220, LigI (gil374074685), and BmulJ_04915 (L-fucono-1,5-lactonase). Residues highlighted in maroon are conserved active site residues important for catalysis. Black arrows represent β -strands that make up the $(\beta/\alpha)_8$ -barrel.

s^{-1} . The next best substrate, L-glucose (7), is oxidized 3 orders of magnitude less efficiently. The L-galactono-1,5-lactone (11) is chemically unstable and rapidly isomerizes to L-galactono-1,4-lactone (2). We suggest that Bvu0219 be called L-galactose dehydrogenase and that the corresponding gene be designated as *lgaA*. In the subsequent step, Bvu0220 hydrolyzes L-galactono-1,5-lactone (11) to L-galactonate (13). The substrate specificity of Bvu0220 is broader than that of Bvu0219, but the two 1,5-lactones (L-glucono-1,5-lactone (1) and 4-deoxy-L-fucono-1,5-lactone (12)) are hydrolyzed about an order of

magnitude faster than any of the 1,4-lactones, including L-galactono-1,4-lactone (2). However, the clear preference for the hydrolysis of L-galactono-1,5-lactone (11) by Bvu0220 was demonstrated with NMR spectroscopy using Bvu0219 to rapidly oxidize [^{13}C -1]-L-galactose to L-galactono-1,5-lactone (11). We suggest that this enzyme be named L-galactono-1,5-lactonase and the corresponding gene be denoted as *lgaB*. In the final step, Bvu0222 oxidizes L-galactonate (13) at C-5 to form D-tagaturonate (16). We propose that Bvu0222 be called L-galactonate dehydrogenase and the gene that encodes this

protein be labeled as *IgaC*. The overall reaction pathway is presented in Scheme 5.

Metabolism of D-Tagaturonate. What is the probable fate of D-tagaturonate? In bacteria such as *E. coli*, the keto group at C2 of D-tagaturonate (16) is reduced to form D-altronate (18) by UxaB, followed by the UxaA catalyzed dehydration of D-altronate to 2-keto-3-deoxygluconate (KDG) (19). This product is then phosphorylated by KDG kinase (KdgK) to form 2-keto-3-deoxygluconate-6-phosphate (20) and then cleaved by an aldolase (KdgA) to generate pyruvate and D-glyceraldehyde-3-phosphate. These steps are illustrated in Scheme 6. In *B. vulgatus*, the four proteins needed for the metabolism of D-tagaturonate can be identified with high probability based on their sequence similarity to the experimentally characterized enzymes from *E. coli*. Bvu3075 is 46% identical to D-tagaturonate reductase (UxaB), Bvu3053 is 46% identical to D-altronate dehydratase (UxaA), Bvu3055 is 25% identical to KdgK and Bvu3056 is 33% identical to KdgA. Therefore, it appears that *B. vulgatus* can metabolize L-galactose to pyruvate and D-glyceraldehyde by a pathway that consists of seven steps.

Bvu0219 and Other Enzymes in cog0667. Experimentally verified members of cog0667 include the following enzymes: L-glyceraldehyde phosphate reductase, D-arabinose dehydrogenase, L-fucose dehydrogenase, and L-galactose dehydrogenase.^{24,30–32} As previously mentioned, Bvu0219 shares approximately 42% sequence identity with L-galactose dehydrogenase from *A. thaliana*. We have predicted that at least 35 proteins in the NCBI protein database share the same substrate profile as Bvu0219. This prediction is based on significant sequence identity (>40%) and if the protein of interest is encoded adjacent to homologues of Bvu0220 and Bvu0222.

Bvu0220 and Other Enzymes in cog3618. We have previously determined the three-dimensional structures of two enzymes from cog3618, FucL (PDB id: 4DNM) and LigI (PDB id: 4D8L). LigI catalyzes the hydrolysis of 2-pyrone-4,6-dicarboxylate in the degradation of lignin. Bvu0220 shares approximately 28% and 15% sequence identity with FucL and LigI, respectively. Despite the relatively low sequence identity to other members of cog3618, Bvu0220 conserves important catalytic active site residues (Figure 5). These include the HxH motif from β -strand 1, histidine from β -strand 6, arginine from β -strand 4, and aspartate from β -strand 8. A total of 12 proteins in the SSN for cog3618 (Figure 2) are predicted to share the same substrate profile as Bvu0220. In addition, there are approximately 35 proteins in the NCBI protein database (not represented in the SSN) that are predicted to share this substrate profile (Table S1, Supporting Information).

Bvu0222 and Other Enzymes in cog1063. Cog1063 contains primarily oxidoreductase enzymes including D-glucose dehydrogenase, L-idonate dehydrogenase, L-arabinitol dehydrogenase, L-threonine dehydrogenase, D-xylulose dehydrogenase, sorbitol dehydrogenase, and L-gluconate dehydrogenase.^{33–39} As mentioned, the closest homologue of verified function is L-gluconate dehydrogenase (LgnH) from *Paracoccus sp.* 43P, which shares 46% sequence identity. LgnH was reported to oxidize both L-gluconate and L-galactonate with k_{cat}/K_m values $> 10^4 \text{ M}^{-1} \text{ s}^{-1}$. Conversely, Bvu0222 oxidizes L-galactonate with a k_{cat}/K_m value approximately 2 orders of magnitude greater than that for L-gluconate. As many as 35 protein sequences have been identified within the NCBI database and predicted to

share the same substrate profile as Bvu0222 (Table S3, Supporting Information).

Metabolic Pathways for L-Galactose. L-Galactose is most notable as an intermediate in the biosynthesis of ascorbic acid in higher plants. For ascorbic acid biosynthesis, L-galactose is produced through a series of reactions, beginning with D-glucose-6-phosphate, which is ultimately converted to GDP-D-mannose. GDP-D-mannose is then transformed to GDP-L-galactose through epimerization at C3 and C4 of the sugar moiety. Phosphorolysis of this product yields GDP and L-galactose-1-phosphate, which is subsequently dephosphorylated to L-galactose.²⁷ L-Galactose was first isolated from flaxseed oil in 1903, and it was later identified to be a component of certain pectins.⁴¹ Since then, L-galactose has been identified as a component of agar, galactagen, agaropectin, and rhamnogalacturonan II (RG-II).⁴¹ RG-II is a structural component of plant cell walls, which makes up approximately 10% of the total pectin in the biosphere. 6-Deoxy-L-galactose (L-fucose) is a known component of RG-II. It has recently been discovered that L-galactose is naturally substituted for L-fucose in RG-I.⁴¹ For example, 24% of RG-II in red wine and 14% in carrots (*Daucus carota*) is substituted with L-galactose.

This is the first pathway described for the transformation of L-galactose to D-tagaturonate. Bioinformatics analysis reveal this pathway to be prevalent in many *Bacteroides* species as well as in other gut microbes, such as *Paraprevotella clara*, *Parabacteroides goldsteinii*, *Paraprevotella xylaniphila*, and *Parabacteroides sp.* CAG:409. In addition to gut microbes, the pathway is found in *Prevotella paludivivens* and *Proteiniphilum acetatigenes* isolated from a rice field in Japan and brewery wastewater, respectively.

Discovery of Novel Metabolic Pathways. In this investigation we identified and characterized a novel pathway for the metabolism of L-galactose in bacteria that reside within the human gut. This discovery was initiated by the comprehensive application of bioinformatics and sequence similarity networks for the identification of enzymes of unknown function that are homologues to previously characterized lactonases from the amidohydrolase superfamily in cog3618. The gene for one of these enzymes of unknown function, Bvu0220, was found clustered in an apparent operon for carbohydrate metabolism. The catalytic properties of this enzyme were elucidated through the utilization of a small, but focused, library of potential sugar lactones. Sequence similarity networks and small physical libraries of potential substrates were strategically utilized to identify substrate profiles for two other enzymes of unknown function in this putative operon for the metabolism of L-galactose. Similar strategies can be readily applied in a broader effort to annotate previously uncharacterized metabolic pathways.

■ ASSOCIATED CONTENT

📄 Supporting Information

Tables S1, S2, and S3. This material is available free of charge via the Internet at <http://pubs.acs.org>.

■ AUTHOR INFORMATION

Corresponding Author

*Telephone: 979-845-3373; e-mail: raushel@tamu.edu.

Funding

This work was supported in part by the Robert A. Welch Foundation (A-840) and the National Institutes of Health (GM 71790 and GM 94662).

Notes

The authors declare no competing financial interest.

ABBREVIATIONS

AHS, amidohydrolase superfamily; LigI, 2-pyrone-4,6-dicarboxylate; FucL, L-fucono-1,5-lactonase; FucD, L-fucose dehydrogenase; SSN, sequence similarity network; IPTG, isopropyl β -D-1-thiogalactopyranoside; PMSF, phenylmethylsulfonyl fluoride; KDG, 2-keto-3-deoxygluconate; KdgK, KDG kinase; KdgA, 2-keto-3-deoxygluconate-6-phosphate aldolase

REFERENCES

(1) Xu, J., Mahowald, M. A., Ley, R. E., Lozupone, C. A., Hamady, M., Martens, E. C., Henrissat, B., Coutinho, P. M., Minx, P., Latreille, P., Cordum, H., Van Brunt, A., Kim, K., Fulton, R. S., Fulton, L. A., Clifton, S. W., Wilson, R. K., Knight, R. D., and Gordon, J. I. (2007) Evolution of symbiotic bacteria in the distal human intestine. *PLoS Biol.* 5, e156.

(2) Saitoh, S., Noda, S., Aiba, Y., Takagi, A., Sakamoto, M., Benno, Y., and Koga, Y. (2002) *Bacteroides ovatus* as the predominant commensal intestinal microbe causing a systemic antibody response in inflammatory bowel disease. *Clin. Vac. Immunol.* 9, 54–59.

(3) Wexler, H. M. (2007) *Bacteroides* the good, the bad, and the nitty-gritty. *Clin. Microbiol. Rev.* 20, 593–621.

(4) Xu, J., Bjursell, M. K., Himrod, J., Deng, S., Carmichael, L. K., Chiang, H. C., Hooper, L. V., and Gordon, J. I. (2003) A genomic view of the human-*Bacteroides thetaiotaomicron* symbiosis. *Science* 299, 2074–2076.

(5) Hooper, L. V., Midtvedt, T., and Gordon, J. I. (2002) How host-microbial interactions shape the nutrient environment of the mammalian intestine. *Annu. Rev. Nutr.* 22, 283–307.

(6) Seibert, C. M., and Raushel, F. M. (2005) Structural and catalytic diversity within the amidohydrolase superfamily. *Biochemistry* 44, 6383–6391.

(7) Ghodge, S. V., Fedorov, A. A., Fedorov, E. V., Hillerich, B., Seidel, R., Almo, S. C., and Raushel, F. M. (2013) Structural and mechanistic characterization of L-histidinol phosphate phosphatase from the polymerase and histidinol phosphatase family of proteins. *Biochemistry* 52, 1101–1112.

(8) Hara, H., Masai, E., Katayama, Y., and Fukuda, M. (2000) The 4-Oxalomesaconate hydratase gene, involved in the protocatechuate 4,5-cleavage pathway, is essential to vanillate and syringate degradation in *Sphingomonas paucimobilis* SYK-6. *J. Bacteriol.* 182, 6950–6957.

(9) Peng, X., Masai, E., Kitayama, H., Harada, K., Katayama, Y., and Fukuda, M. (2002) Characterization of the 5-carboxyvanillate decarboxylase gene and its role in lignin-related biphenyl catabolism in *Sphingomonas paucimobilis* SYK-6. *Appl. Environ. Microbiol.* 68, 4407–4415.

(10) Hitchcock, D. S., Fedorov, A. A., Fedorov, E. V., Dangott, L. J., Almo, S. C., and Raushel, F. M. (2011) Rescue of the orphan enzyme isoguanine deaminase. *Biochemistry* 50, 5555–5557.

(11) Halak, S., Basta, T., Buerger, S., Contzen, M., Wray, V., Pieper, D. H., and Stolz, A. (2007) 4-sulfomuconolactone hydrolases from *Hydrogenophaga intermedia* S1 and *Agrobacterium radiobacter* S2. *J. Bacteriol.* 189, 6998–7006.

(12) Hobbs, M. E., Malashkevich, V., Williams, H. J., Xu, C., Sauder, J. M., Burley, S. K., Almo, S. C., and Raushel, F. M. (2012) Structure and catalytic mechanism of LigI: insight into the amidohydrolase enzymes of cog3618 and lignin degradation. *Biochemistry* 51, 3497–3507.

(13) Hobbs, M. E., Vetting, M., Williams, H. J., Narindoshvili, T., Kebodeaus, D. M., Hillerich, B., Seidel, R. D., Almo, S. C., and Raushel,

F. M. (2013) Discovery of an L-fucono-1,5-lactonase from cog3618 of the amidohydrolase superfamily. *Biochemistry* 52, 239–253.

(14) Xiang, D. F., Kolb, P., Fedorov, A. A., Xu, C., Fedorov, E. V., Narindoshvili, T., Williams, H. J., Shoichet, B. K., Almo, S. C., and Raushel, F. M. (2012) Structure-based function discovery of an enzyme for the hydrolysis of phosphorylated sugar lactones. *Biochemistry* 51, 1762–1773.

(15) Savitsky, P., Bray, J., Cooper, C. D. O., Marsden, B. D., Mahajan, P., Burgess-Brown, N. A., and Gileadi, O. (2010) High-throughput production of human proteins for crystallization: The SGC experience. *J. Struct. Biol.* 172, 3–13.

(16) Schenk, P. M., Baumann, S., Mattes, R., and Steinbiss, H. H. (1995) Improved high-level expression system for eukaryotic genes in *Escherichia coli* using T7 RNA polymerase and rare ArgtRNAs. *BioTechniques* 19, 196–180.

(17) Williams, L., Nguyen, T., Li, Y. C., Porter, T. N., and Raushel, F. M. (2006) Uronate isomerase: a nonhydrolytic member of the amidohydrolase superfamily with an ambivalent requirement for a divalent metal ion. *Biochemistry* 45, 7453–7462.

(18) Hall, R. S., Fedorov, A. A., Marti-Arbona, R., Fedorov, E. V., Kolb, P., Sauder, J. M., Burley, S. K., Shoichet, B. K., Almo, S. C., and Raushel, F. M. (2010) The hunt for 8-oxoguanine deaminase. *J. Am. Chem. Soc.* 132, 1762–1763.

(19) Hall, R. S., Agarwal, R., Hitchcock, D., Sauder, J. M., Burley, S. K., Swaminathan, S., and Raushel, F. M. (2010) Discovery and structure determination of the orphan enzyme isoxanthopterin deaminase. *Biochemistry* 49, 4374–4382.

(20) Atkinson, H. J., Morris, J. H., Ferrin, T. E., and Babbitt, P. C. (2009) Using sequence similarity networks for visualization of relationships across diverse protein superfamilies. *PLoS One* 4, e4345.

(21) Smoot, M. E., Ono, K., Ruschinski, J., Wang, P.-L., and Ideker, T. (2011) Cytoscape 2.8: new features for data integration and network visualization. *Bioinformatics* 27, 431–432.

(22) Waterhouse, A. M., Procter, J. B., Martin, D. M. A., Clamp, M., and Barton, G. J. (2009) Jalview version 2—a multiple sequence alignment editor and analysis workbench. *Bioinformatics* 25, 1189–1191.

(23) Zhu, Y., and Lin, E. C. (1987) Loss of aldehyde dehydrogenase in an *Escherichia coli* mutant selected for growth on the rare sugar L-galactose. *J. Bacteriol.* 169, 785–789.

(24) Gatzek, S., Wheeler, G. L., and Smirnov, N. (2002) Antisense suppression of L-galactose dehydrogenase in *Arabidopsis thaliana* provides evidence for its role in ascorbate synthesis and reveals light modulated L-galactose synthesis. *Plant J.: Cell Mol. Biol.* 30 (5), 541–553.

(25) Mieda, T., Yabuta, Y., Rapolu, M., Motoki, T., Takeda, T., Yoshimura, K., Ishikawa, T., and Shigeoka, S. (2004) Feedback inhibition of spinach L-galactose dehydrogenase by L-ascorbate. *Plant Cell Physiol.* 45, 1271–1279.

(26) Momma, M., and Fujimoto, Z. (2013) Expression, crystallization and preliminary X-ray analysis of rice L-galactose dehydrogenase. *Acta Crystallogr.* 69, 809–811.

(27) Imai, T., Ban, Y., Terakami, S., Yamamoto, T., and Moriguchi, T. (2009) L-Ascorbate biosynthesis in peach: cloning of six L-galactose pathway-related genes and their expression during peach fruit development. *Physiol. Plant.* 136, 139–149.

(28) Angyal, S. J., Bethell, G. S., Cowley, D. E., and Pickles, V. A. (1976) Equilibria between pyranoses and furanoses. IV. 1-Deoxyhexuloses and 3-hexuloses. *Aust. J. Chem.* 29, 1239–1247.

(29) Shimizu, T., Takaya, N., and Nakamura, A. (2012) An L-glucose catabolic pathway in *Paracoccus species* 43P. *J. Biol. Chem.* 287, 40448–40456.

(30) Desai, K. K., and Miller, B. G. (2008) A metabolic bypass of the triosephosphate isomerase reaction. *Biochemistry* 47, 7983–7985.

(31) Amako, K., Fujita, K., Shimohata, T. A., Hasegawa, E., Kishimoto, R., and Goda, K. (2006) NAD⁺-specific D-arabinose dehydrogenase and its contribution to erythroascorbic acid production in *Saccharomyces cerevisiae*. *FEBS Lett.* 580, 6428–6443.

(32) Yew, W. S., Fedorov, A. A., Fedorov, E. V., Rakus, J. F., Pierce, R. W., Almo, S. C., and Gerlt, J. A. (2006) Evolution of enzymatic activities in the enolase superfamily: L-fuconate dehydratase from *Xanthomonas campestris*. *Biochemistry* 45, 14582–14597.

(33) Nobelmann, B., and Lengeler, J. W. (1995) Sequence of the gat operon for galactitol utilization from a wild-type strain EC3132 of *Escherichia coli*. *BBA-Gene Struct Expr.* 1262, 69–72.

(34) Angelov, A., Futterer, O., Valerius, O., Braus, G. H., and Liebl, W. (2005) Properties of the recombinant glucose/galactose dehydrogenase from the extreme thermoacidophile. *Picrophilus torridus*. *FEBS J.* 272, 1054–1062.

(35) Smith, L. D., Budgen, N., Bungard, S. J., Danson, M. J., and Hough, D. W. (1989) Purification and characterization of glucose dehydrogenase from the thermoacidophilic archaeobacterium *Thermoplasma acidophilum*. *Biochem. J.* 261, 973–977.

(36) DeBolt, S., Cook, D. R., and Ford, C. M. (2006) L-Tartaric acid synthesis from vitamin C in higher plants. *P Natl. Acad. Sci. USA* 103, 5608–5613.

(37) Epperly, B. R., and Dekker, E. E. (1991) L-Threonine dehydrogenase from *Escherichia coli*. *J. Biol. Chem.* 266, 6086–6092.

(38) Aguayo, M. F., Ampuero, D., Mandujano, P., Parada, R., Munoz, R., Gallart, M., Altabella, T., Cabrera, R., Stange, C., and Handford, M. (2013) Sorbitol dehydrogenase is a cytosolic protein required for sorbitol metabolism in *Arabidopsis thaliana*. *Plant Sci.* 205, 63–75.

(39) Kim, B., Sullivan, R. P., and Zhao, H. M. (2010) Cloning, characterization, and engineering of fungal L-arabinitol dehydrogenases. *Appl. Microbiol. Biotechnol.* 87, 1407–1414.

(40) Anderson, E. (1933) The preparation of L-galactose from flaxseed mucilage. *J. Biol. Chem.* 100, 249–253.

(41) Pabst, M., Fischl, R. M., Brecker, L., Morelle, W., Fauland, A., Kofeler, H., Altmann, F., and Leonard, R. (2013) Rhamnogalacturonan II structure shows variation in the side chains monosaccharide composition and methylation status within and across different plant species. *Plant J.: Cell Mol. Biol.* 76, 61–72.